Isotope Specific Resolution Modelling Image Reconstruction for High Resolution PET Imaging

Fotis A. Kotasidis, *Member IEEE*, Jose M. Anton-Rodriguez, Georgios I. Angelis, *Member IEEE*, Julian C. Matthews, Andrew J Reader, *Member IEEE*, Habib Zaidi, *Senior Member, IEEE*

Abstract— **Measuring the spatially variant point spread function (PSF) on a PET scanner involves using a point source to sample the field of view (FOV) at multiple locations. However, since most clinically used isotopes have short half-lives, usually other non-clinically used long-lived isotopes are employed in practice. As such, due to the difference in positron range, non-optimal PSF models that do not correspond to those needed for the data to be reconstructed, are used within resolution modelling (RM) image reconstruction, usually underestimating the true PSF. In our previous work, the spatially variant PSF was measured on the HRRT based on clinically used isotopes. Here we extend the work by evaluating the impact of using isotope-specific PSF maps within RM image reconstruction. Evaluation is performed using point source, phantom and clinical datasets. Results suggest that further improvements in spatial resolution and contrast can be obtained by using an isotope-specific PSF.**

Index Terms—**PSF reconstruction, positron range, HRRT**

I. INTRODUCTION

Resolution recovery image reconstruction algorithms in PET imaging have been shown to improve both signal to noise ratio as well as spatial resolution, leading to more accurate quantification. Despite the added complexity of such algorithms their aforementioned attributes have led recently to their introduction in most clinically used scanners. Derivation and implementation of the PSF in projection space constitutes the most accurate approach, but due to the finite number of measurements as well as the subsequent response parameterization and further interpolation, image based techniques can yield similar results [1]. Whether implemented in image or projection space, these algorithms are usually based on an accurate estimation of the spatially invariant or variant PSF obtained from measured point source data [2-4]. However these measurements are usually performed based on long-lived isotopes not typically used in clinical practice [2, 5]. As such, with the measured kernels being positron range dependant, the PSF models used within image reconstruction do not correspond to the actual blurring in the measured data usually under-estimating the true PSF and leading to suboptimal resolution recovery during reconstruction. In whole body scanners, were spatial resolution is dominated by scanner specific resolution degrading effects, the PSF is less susceptible upon changes in the isotope's positron range. However in high resolution brain and pre-clinical imaging the overall spatial resolution becomes positron range limited with potentially substantial benefits to be gained from using isotope specific kernels within RM image reconstruction. In our previous work using a printing point source technique which enables simultaneous evaluation of the spatial variant PSF at multiple locations in the FOV, we demonstrated the feasibility of deriving isotope specific PSFs from clinically used positron emitting isotopes using the high resolution research tomograph (HRRT) [6-8]. Extending this work and using a recently implemented spatially variant resolution modelling (SVRM) reconstruction for the HRRT based on the ordinary Poisson ordered subsets expectation maximization algorithm (OPOSEM), we evaluate the impact of isotope dependant PSFs within image reconstruction [9].

F.A.Kotasidis is with the Division of Nuclear Medicine & Molecular Imaging, Geneva University Hospital, Geneva, Switzerland and with the Wolfson Molecular Imaging Centre, MAHSC, University of Manchester, Manchester UK
J.C. Matthews and Jose M. Anton-Rodriguez *are* with the Wolfson Molecular Imaging Centre, MAHSC, University of Manchester, Manchester UK
G. I.Angelis is with the Brain and Mind Institute, University of Sydney, Sydney, Australia
A.J.Reader is with the Department of Biomedical Engineering, Division of Imaging Sciences and Biomedical Engineering, King's College London, St. Thomas' Hospital, London, UK and Montreal Neurological Institute,McGill University, Montreal, Canada
Habib Zaidi is with the Division of Nuclear Medicine and Molecular Imaging, Geneva University Hospital, the Geneva Neuroscience Center, Geneva University, Geneva, Switzerland and the Department of Nuclear Medicine and Molecular Imaging, University of Groningen, University Medical Center Groningen, Groningen, The Netherlands

II. METHODS

The spatially variant PSF was experimentally measured on the HRRT by printing an array of 15 (radially - 18,5 mm spacing) × 11 (axially - 19.5 mm spacing) point sources, 1mm in diameter using fluorine-18 (mean positron range of 0.66 mm) and carbon-11 (mean positron range of 1.266 mm) [10]. Due to the PSF on the HRRT being invariant under axial transformations, the PSF map was generated from averaging the parameters derived across the 11 axial positions. To assess the impact of using isotope-specific PSF compared to the

standard PSF (being non-specific to the isotope of the study to be reconstructed) we used carbon-11 datasets. To assess the spatial resolution characteristics we used carbon-11 point source data and a single scan of the point source array was acquired for 60 minutes collecting 65×10^6 prompts. To evaluate bias-variance performance the Esser image quality phantom was scanned and analysed to the NEMA specifications [11]. The 8,12,16 and 25 mm cylinders were filled with carbon-11 with a 4:1 ratio over the warm background. Two 25 mm cylinders were left empty and along with a 25mm solid cylinder represented cold regions. Data were acquired for 120 minutes collecting 8.7×10^8 prompts. Finally a single clinical [^{11}C]methionine dataset from a patient with a grade II oligodendroglioma was used [12]. The patient was injected with 430 MBq of [^{11}C]methionine followed by a 60 minute data acquisition in list-mode and a 6 minute transmission scan for attenuation correction. All datasets were reconstructed using 2 SVRM reconstructions: the one using the fluorine-18 derived PSF map, representing our standard variant PSF map available on the HRRT (non-isotope specific SVRM reconstruction) and the one using the carbon-11 derived PSF map, representing the isotope specific PSF map (isotope specific SVRM reconstruction) [9]. As such the fluorine-18 based SVRM reconstruction should underestimate the true PSF on the carbon-11 datasets compared to the carbon-11 based SVRM reconstruction which should provide a good match. For comparison the datasets were also reconstructed using OPOSEM without RM, as well as with the HRRT user's community spatially invariant RM (SIRM) reconstruction [13-16].

III. RESULTS AND DISCUSSION

Fig 1 shows graphs of contrast recovery (CR) versus image roughness (IR) for the 25mm hot (i) and cold (ii) sphere for up to 20 iterations (16 subsets) as well as images of the Esser phantom (at matched IR level) for all 4 reconstructions. In the cold sphere, the carbon-11 SVRM reconstruction has a ~94% CR at the 20th iteration compared to ~92% for the fluorine-18 SVRM at the same variance level. In the hot sphere no significant difference can be seen between the 2 SVRM reconstructions. The carbon-11 SVRM method converges more slowly due to the broader PSF kernels and probably more than 20 iterations are needed to see potentially improved bias variance performance. However this is to be expected as the cylinders in the Esser phantom are not centrally located (~7cm off centre) where the difference between the isotope specific (carbon-11) and non-specific (fluorine-18) RM reconstructions should be more pronounced. Towards the edge of the radial FOV were the parallax error dominates the resolution, the positron range has little impact resulting in the variant PSF maps from the 2 isotopes being comparable and the respective reconstructions perform similarly. Reconstructed images of the clinical [^{11}C]methionine dataset are shown in Fig. 2 for all methods, as well as the difference between the isotope specific and non-specific RM reconstructions (carbon-11 - fluorine-18). Increased contrast is obtained in the carbon-11 SVRM reconstruction looking at
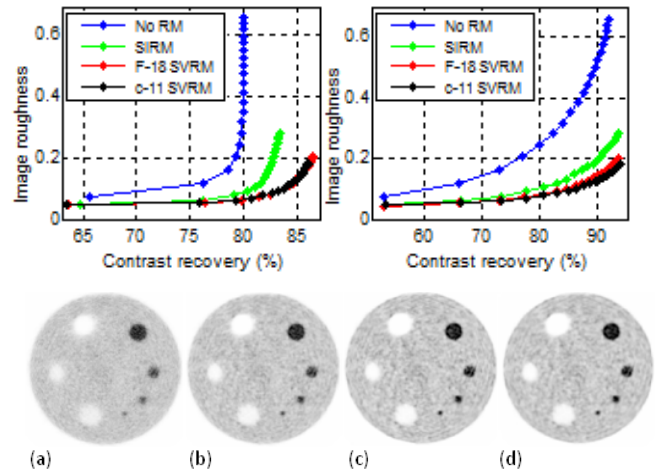

Fig.1 Graphs of contrast recovery (CR) versus image roughness (IR) for the 25 mm hot (top left) and cold (top right) cylinder as well as images of the Esser phantom using (a) no RM, (b) HRRT user's SIRM, (c) Fluorine-18 SVRM, and (d) the Carbon-11 SVRM reconstruction at matched variance level.
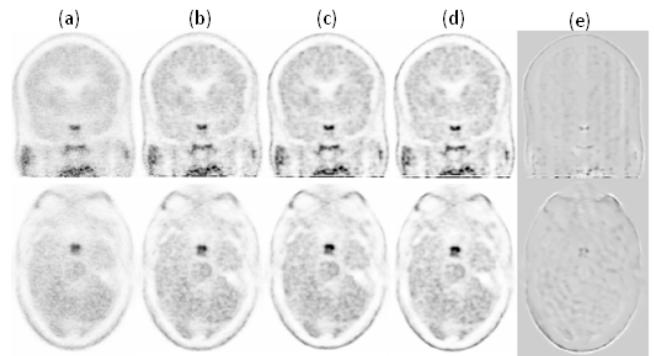

Fig. 2 Clinical data reconstructed with (a) no RM, (b) HRRT user's SIRM, (c) Fluorine-18 SVRM, and (d) the Carbon-11 SVRM while (e) is the difference between (d) minus (c).Images shown at same variance level based on Fig. 1

their difference, with the improvements located at the boundaries of regions with high activity gradient and with a peak uptake difference in the tumour of 1-1.5%. Finally profiles from the reconstructed carbon-11 point sources are plotted in Fig. 3 (20th iteration). Resolution recovery is more pronounced using the carbon-11 SVRM reconstruction despite its slower convergence compared to the fluorine-18 SVRM reconstruction. However at the 20th iteration all reconstructions have almost converged (after 15th iteration no significant change was seen) showing the improved resolution characteristics obtained by using the isotope specific PSF within the reconstruction.

IV. CONCLUSION

Improved images can be obtained using RM reconstruction algorithms with PSF maps specific to the isotope of the study
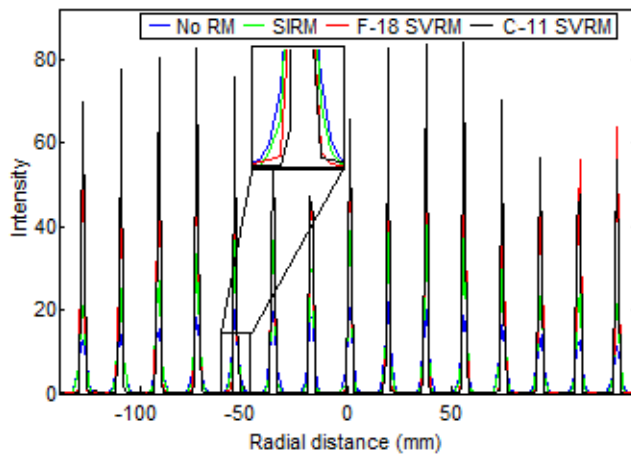
Fig. 3 Profiles from the point source data reconstructed with all methods.

to be reconstructed. These improvements depend on the positron range difference between the isotope used to derive the standard PSF maps used by the scanner and the isotope used in the study to be reconstructed. In our investigation we used carbon-11 datasets and as we selected the fluorine-18 PSF to represent the standard PSF map, the improvements obtained by using the carbon-11 PSF are modest. More significant benefits are expected to be gained in studies using water-15 or rubidium-82 based tracers by using isotope specific PSFs within reconstruction.

V. REFERENCES

[1] F. A. Kotasidis, J. C. Matthews, G. I. Angelis, P. J. Noonan, A. Jackson, P. Price, *et al.*, "Single scan parameterization of space-variant point spread functions in image space via a printed array: the impact for two PET/CT scanners.," *Phys Med Biol,* vol. 56, pp. 2917-2942, May 21 2011.

[2] V. Y. Panin, F. Kehren, C. Michel, and M. Casey, "Fully 3-D PET reconstruction with system matrix derived from point source measurements.," *IEEE Trans Med Imaging,* vol. 25, pp. 907-921, 2006.

[3] D. Wiant, J. A. Gersh, M. Bennett, and J. D. Bourland, "Evaluation of the spatial dependence of the point spread function in 2D PET image reconstruction using LOR-OSEM.," *Med Phys,* vol. 37, pp. 1169-1182, 2010.

[4] A. M. Alessio, C. W. Stearns, S. Tong, S. G. Ross, S. Kohlmyer, A. Ganin, *et al.*, "Application and evaluation of a measured spatially variant system model for PET image reconstruction.," *IEEE Trans Med Imaging,* vol. 29, pp. 938-949, 2010.

[5] C. Cloquet, F. C. Sureau, M. Defrise, G. Van Simaeys, N. Trotta, and S. Goldman, "Non-Gaussian space-variant resolution modelling for list-mode reconstruction.," *Phys Med Biol,* vol. 55, pp. 5045-5066, 2010.

[6] F. A. Kotasidis, G. I. Angelis, J. Anton-Rodriguez, J. C. Matthews, A. J. Reader, M. Green, *et al.*, "Isotope dependent system matrices for high resolution PET imaging," in *Nuclear Science Symposium and Medical Imaging Conference (NSS/MIC), 2012 IEEE*, 2012, pp. 2925-2928.

[7] F. A. Kotasidis, G. I. Angelis, J. Henderson, A. Buckley, P. J. Markiewicz, M. Green, *et al.*, "Evaluation of image based spatially variant and count rate dependant point spread functions on the HRRT PET scanner," in *Nuclear Science Symposium and Medical Imaging Conference (NSS/MIC), 2011 IEEE*, 2011, pp. 3595-3596.

[8] P. J. Markiewicz, G. I. Angelis, F. Kotasidis, M. Green, W. R. Lionheart, A. J. Reader, *et al.*, "A custom-built PET phantom design for quantitative imaging of printed distributions.," *Phys Med Biol,* vol. 56, pp. N247-261, Nov 7 2011.

[9] G. I. Angelis, F. A. Kotasidis, J. C. Matthews, P. J. Markiewicz, W. R. Lionheart, and A. J. Reader, "Full field spatially-variant image-based resolution modelling reconstruction for the HRRT," in *Nuclear Science Symposium and Medical Imaging Conference (NSS/MIC), 2012 IEEE*, 2012, pp. 3434-3438.

[10] L. Jodal, C. Le Loirec, and C. Champion, "Positron range in PET imaging: an alternative approach for assessing and correcting the blurring," *Phys Med Biol,* vol. 57, pp. 3931-43, Jun 21 2012.

[11] M. E. Daube-Witherspoon, J. S. Karp, M. E. Casey, F. P. DiFilippo, H. Hines, G. Muehllehner, *et al.*, "PET performance measurements using the NEMA NU 2-2001 standard.," *J Nucl Med,* vol. 43, pp. 1398-1409, Oct 2002.

[12] D. J. Coope, J. Cizek, C. Eggers, S. Vollmar, W. D. Heiss, and K. Herholz, "Evaluation of primary brain tumors using 11C-methionine PET with reference to a normal methionine uptake map," *J Nucl Med,* vol. 48, pp. 1971-80, Dec 2007.

[13] I. K. Hong, S. T. Chung, H. K. Kim, Y. B. Kim, Y. D. Son, and Z. H. Cho, "Ultra fast symmetry and SIMD-based Projection-Backprojection (SSP) algorithm for 3-D PET image reconstruction.," *IEEE Trans Med Imaging,* vol. 26, pp. 789-803, 2007.

[14] F. C. Sureau, A. J. Reader, C. Comtat, C. Leroy, M.-J. Ribeiro, I. Buvat, *et al.*, "Impact of image-space resolution modeling for studies with the High-Resolution Research Tomograph.," *J Nucl Med,* vol. 49, pp. 1000-1008, June 1, 2008 2008.

[15] C. Comtat, F. Bataille, C. Michel, J. P. Jones, M. Sibomana, L. Janeiro, *et al.*, "OSEM-3D reconstruction strategies for the ECAT HRRT," in *Nuclear Science Symposium Conference Record, 2004 IEEE*, 2004, pp. 3492-3496 Vol. 6.

[16] A. J. Reader, P. J. Julyan, H. Williams, D. L. Hastings, and J. Zweit, "EM algorithm system modeling by image-space techniques for PET reconstruction," *Nuclear Science, IEEE Transactions on,* vol. 50, pp. 1392-1397, 2003.